American Mineralogist, Volume 61, pages 913–920, 1976

Orientation of exsolved pentlandite in natural and synthetic nickeliferous pyrrhotite

CARL A. FRANCIS[1], MICHAEL E. FLEET[2], KULA MISRA[3], AND JAMES R. CRAIG[1]

[1]*Department of Geological Sciences, Virginia Polytechnic Institute and State University, Blacksburg, Virginia 24061*
[2]*Department of Geology, The University of Western Ontario, London, Ontario N6A3K7*
[3]*Department of Geological Sciences, The University of Tennessee, Knoxville, Tennessee 37916*

Abstract

Pentlandite (pn), $(Fe, Ni)_9S_8$, exsolves from nickeliferous pyrrhotite (po), $(Fe, Ni)_{1-x}S$, in the form of flames exhibiting weak reflection anisotropism and preferred orientation. X-ray precession studies on both natural and synthetic crystals have established the orientation relation: (111)pn|| (00.1)po; $(0\bar{1}1)$pn || (11.0)po; $(\bar{1}\bar{1}2)$pn || (10.0)po. In synthesis experiments, rapidly quenched samples of $(Fe,Ni)_{1-x}S$ solid solutions contain randomly oriented blebs of pentlandite, whereas slowly cooled charges contain coherent lamellae of pentlandite parallel to (00.1) of pyrrhotite.

Introduction

Three textural varieties of pentlandite, $(Fe,Ni)_9S_8$, are common in the pyrrhotite-bearing (Sudbury-type) natural nickel sulfide assemblages: (1) massive (blocky) pentlandite, often containing islands of pyrrhotite; (2) partial to complete rims of pentlandite around pyrrhotite grains; and (3) stringers and blebs of pentlandite in pyrrhotite often showing preferred orientation. "Flame" or "brush" texture, consisting of fine subparallel plates or needles with sharp to ragged borders, is characteristic of the latter variety of pentlandite (Fig. 1), but it also occurs at the margins of rim-type and (more rarely) blocky pentlandite, projecting into the adjacent pyrrhotite. All these textural varieties are often found within the limits of a single polished section; however, detailed electron-microprobe analyses have failed to establish any systematic compositional differences among them.

Crystallization of pentlandite during cooling of synthetic high-temperature $(Fe,Ni)_{1-x}S$ (monosulfide) solid solutions (Newhouse, 1927; Hewitt, 1938; Hawley and Haw, 1957; Kullerud, 1956, 1962), often with textures typical of natural pyrrhotite-pentlandite assemblages, strongly suggests that the pentlandite in natural assemblages has exsolved from a high-temperature nickeliferous pyrrhotite. The withdrawal of the monosulfide solid-solution (mss) solvus in the Fe–Ni–S system to progressively more S-rich compositions at decreasing temperature (Naldrett, *et al.*, 1967; Shewman and Clark, 1970; Misra and Fleet, 1973a), and the fact that the bulk compositions of the typical Sudbury-type Fe–Ni sulfide assemblages lie within the monosulfide solid-solution field at higher temperatures (Naldrett and Kullerud, 1967; Craig and Kullerud, 1969) further supports this interpretation. Thus the subsolidus exsolution origin of pentlandite in nickel-sulfide assemblages is well established.

The present contribution is the combined report of two independent investigations, one on a natural sample by MEF and KCM and the other on synthetic material by CAF and JRC. The crystallographic relationship between host pyrrhotite and exsolved pentlandite is established, correcting previous reports, and structural controls on the exsolution process are discussed.

Oriented intergrowths of several ore-mineral pairs were examined by Gruner (1929), who recognized a common structural feature in them. The arrangement of atoms in one or more atomic layers of the first is nearly identical with that in one or more layers of the second. Further, a single element, usually oxygen or sulfur, populates those layers. For example, there is a close dimensional fit between the oxygen positions in the close-packed (111) layers of magnetite and those in the close-packed (00.1) layers of ilmenite. Such an arrangement, like that of coherent twin boundaries, tends to minimize interfacial energy because the first coordination spheres of the atoms on the common plane are satisfied by both structures (Buerger, 1943; 1945).

Gruner (1929) concluded on the basis of crystal-structural arguments that true "oriented intergrowths

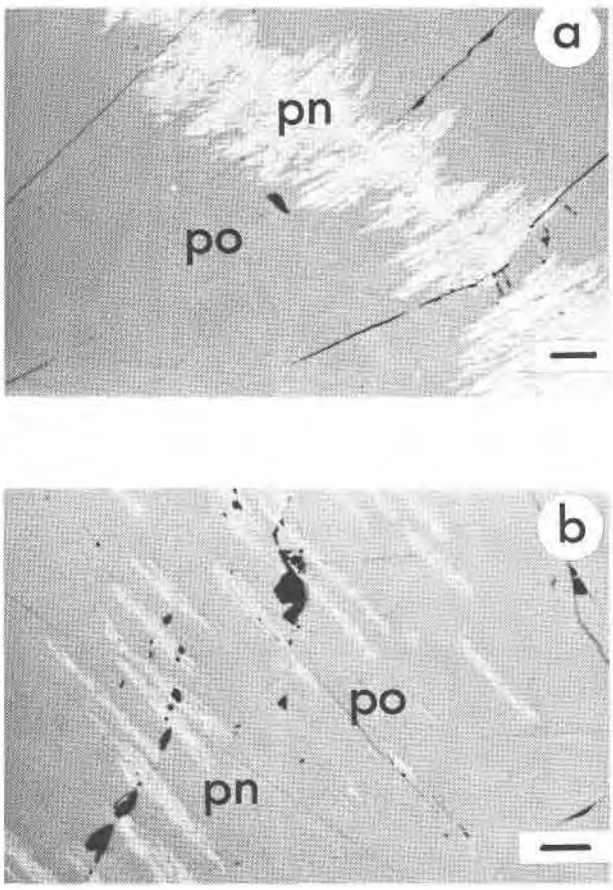

FIG. 1. Photomicrographs illustrating some typical pentlandite (pn)–pyrrhotite (po) textural relationships. The bar in each photomicrograph represents 0.04 mm. Oil immersion, reflected light.
(a) Stringer of flame-textured pentlandite (light gray) in pyrrhotite (darker gray). Note the preferred orientation of the flames parallel to the pyrrhotite cleavage. Specimen 52, Falconbridge mine, Sudbury, Ontario, Canada.
(b) Oriented blebs of flame pentlandite (light gray) in pyrrhotite (darker gray). Specimen 9868, Creighton mine, Sudbury, Ontario, Canada.

of pentlandite and pyrrhotite . . . are improbable if not impossible," despite previous reports of such intergrowths by Newhouse (1927) and others. Subsequently Lindqvist *et al.* (1936) showed that the pentlandite structure determined by Alsén (1925), which formed the basis of Gruner's argument, was incorrect; that structure assumes a unit-cell composition of $8(FeNi_3S_4)$ and has the S and metal positions reversed relative to the accepted structure.

Responding to Gruner's paper, Ehrenberg (1932) documented oriented intergrowths of pentlandite and pyrrhotite. His polished sections from Sudbury show both pentlandite exsolved from pyrrhotite and pyrrhotite exsolved from pentlandite. In the former example, "cut parallel to the base" [presumably the (00.1) of pyrrhotite], pentlandite occurs in three distinct orientations resembling a snowflake. In the later example, apparently hexagonal-shaped pyrrhotite crystals lie in the (111) plane of pentlandite. Ehrenberg also described the only known example of pentlandite epitaxially overgrown on pyrrhotite (Fig. 2). Pentlandite occurs as tri-radiate overgrowths in two orientations on the (00.1) face of pyrrhotite with the rays extending perpendicular to the {10.0} form of pyrrhotite. These "stars" are composed of small crystals that have faces normal to the ray directions and hence parallel to {10.0} of the pyrrhotite substrate. Assuming that the three-fold symmetry of the stars was not merely inherited from the substrate but actually represents that of [111] of pentlandite, Ehrenberg assigned the small vertical faces to the dodecahedron, {110}. He thus deduced that the (111) and (110) planes of pentlandite parallel the (00.1) and (10.0) planes of pyrrhotite respectively [*i.e.* (111) pn ||(00.1)po and (110)pn || (10.0po].

Oriented intergrowths of pentlandite and pyrrho-

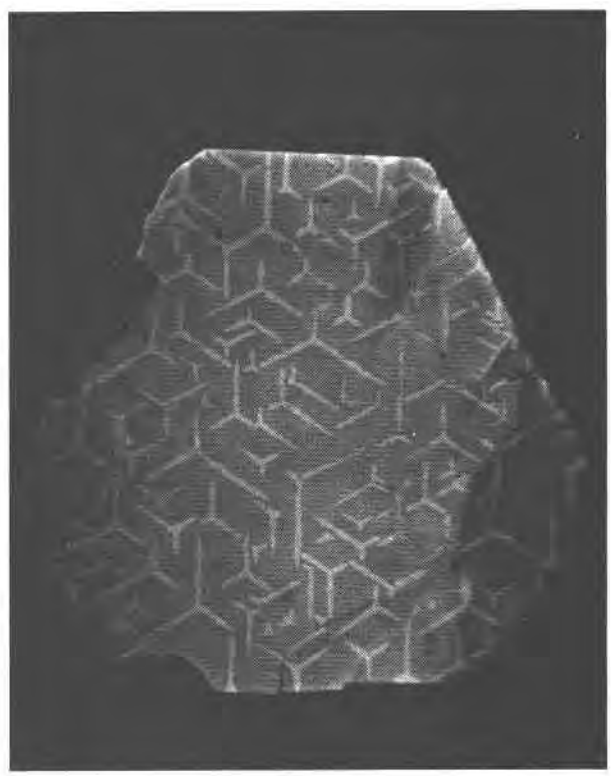

FIG. 2. Pentlandite epitaxially overgrown on pyrrhotite (vertical dimension 2.5 mm) from Miggiadone bei Pallanza, Piemont, Italy (from Ehrenberg, 1932, with permission).

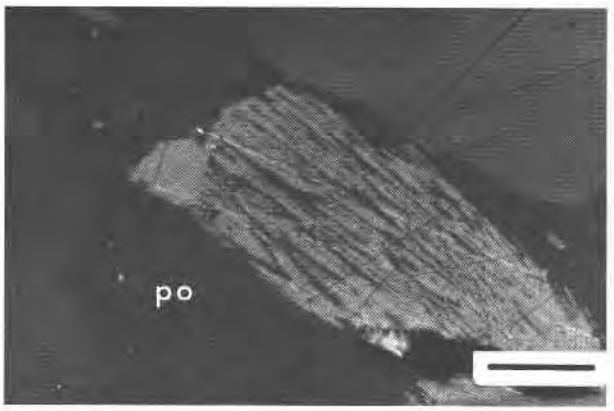

FIG. 3. Photomicrograph of flame-textured pentlandite (light grey) in pyrrhotite showing distinct anisotropism. Analyzer 2° off crossed position, oil immersion, reflected light. Bar is 0.04 mm. Specimen 9868, Creighton mine, Sudbury, Ontario, Canada.

tite are commonly encountered in experimental products as well as in natural samples. They were first produced experimentally by Hawley and Haw (1957) and have subsequently been reproduced by a number of workers (*e.g.* Naldrett *et al.* 1967; Misra, 1972; Craig, 1973).

The crystal structures of both pentlandite and high-temperature pyrrhotite are now well-known. High-temperature pyrrhotite, which is the iron end-member of the mss, has the NiAs structure (Haraldsen, 1941). Lundqvist (1947) confirmed that the mss also has the NiAs structure. Pentlandite was shown to be isostructural with Co_9S_8, by Lindqvist *et al.* (1936) on the basis of powder methods. The structure was confirmed by Pearson and Buerger (1956) and Knop and Ibrahim (1961), and has since been refined by Rajamani and Prewitt (1973).

Experimental methods and results

Natural samples

The specimens used in this portion of the investigation were polished sections from earlier electron-microprobe studies of natural pentlandite assemblages (Misra and Fleet, 1973a, 1974). More detailed examination of the assemblage from the Creighton mine, Sudbury (Specimen 9868) reveals that the flame pentlandite has a weak but distinct reflection anisotropism (Fig. 3) with parallel extinction. As far as we are aware, anisotropic pentlandite has not been reported in the literature. This anisotropism is often masked by the much stronger anisotropism of the enclosing pyrrhotite, but is readily recognized when the microscope analyzer is off-set very slightly from the crossed position. A reexamination of other polished sections from the earlier studies confirms that weak anisotropism is a characteristic feature of the flame pentlandite, and to a lesser extent, of the smaller grains of rim-type pentlandite in these assemblages. When much of the enclosing pyrrhotite is removed, the anisotropism is markedly reduced, suggesting that it results from elastic strain. Such pentlandite is likely to have preserved its original orientation relationship with the host pyrrhotite and was therefore considered ideal for the present study.

A small fragment (about 0.01 mm in longest dimension) of an intergrowth of pyrrhotite and flame pentlandite was removed from a polished section of specimen 9868 and examined by the precession method. A representative X-ray diffraction pattern is shown with an interpretation of the central area of this photograph in Figure 4. The vertical reciprocal lattice row in Figure 4a includes both pyrrhotite (po) 00.*l* and pentlandite (pn) *hhh* diffractions, thus con-

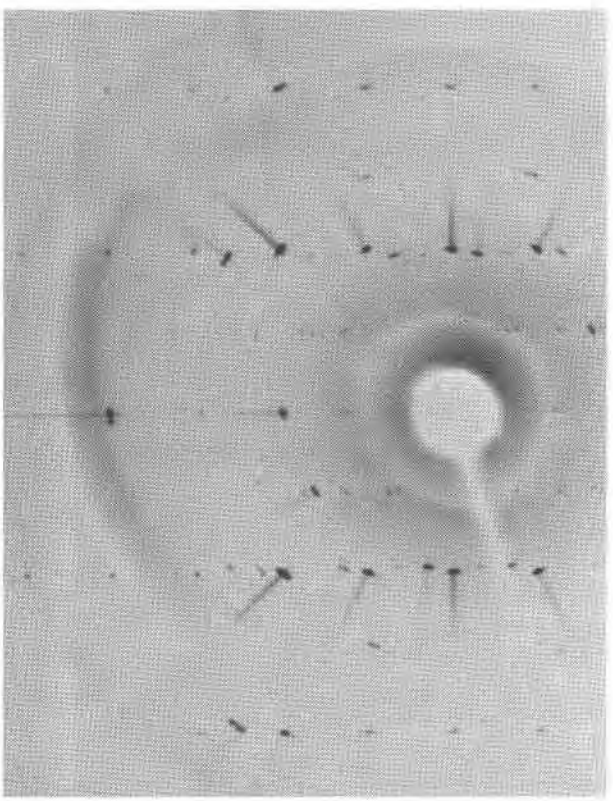

FIG. 4A. Zero level precession photograph showing the crystallographic orientation of pyrrhotite and exsolved pentlandite in specimen 9868. [01.0]po, [1$\bar{1}$0]pn precession axis; μ = 20°; Zr-filtered Mo$K\alpha$ radiation, 35 kV, 20 mA, 14 days exposure.

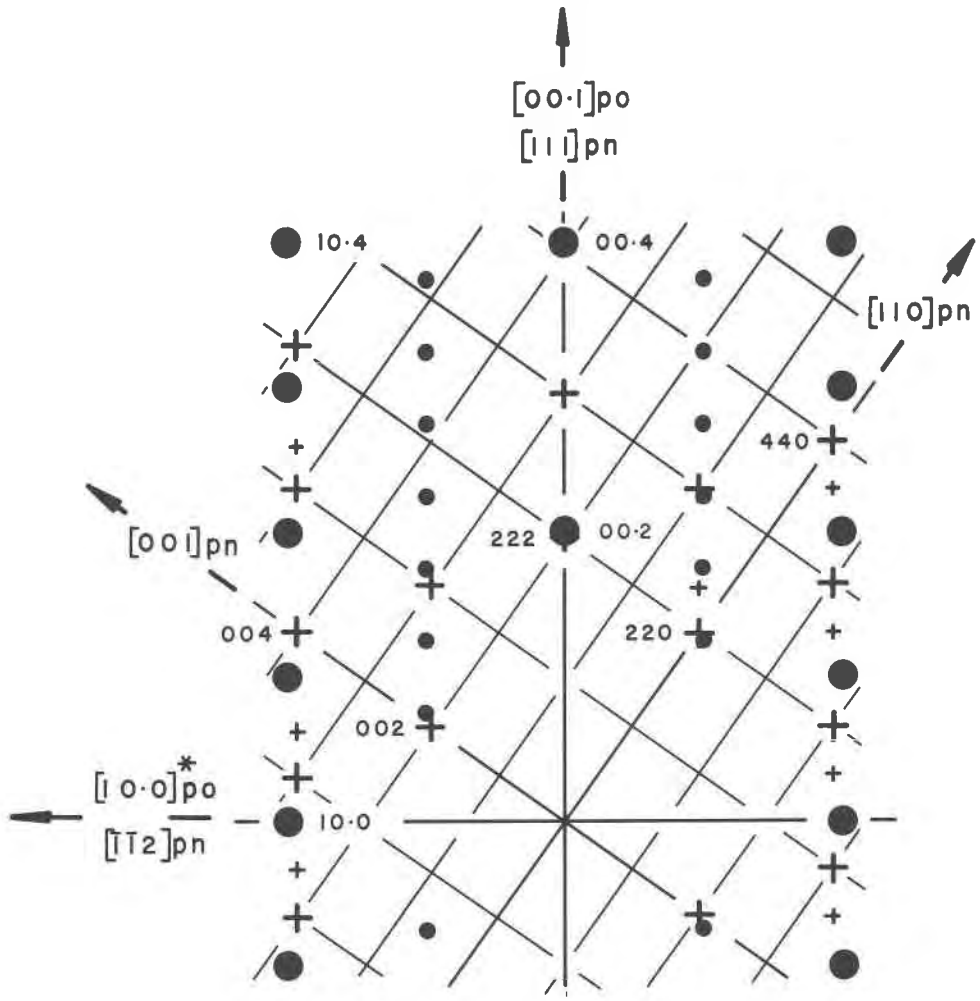

FIG. 4B. Interpretation of the central part of the precession photograph of Fig. 4a. Large solid circles, pyrrhotite (po) subcell reflections; small solid circles, pyrrhotite 4*C* supercell reflections; large plus signs, reflections of pentlandite (pn) in the first orientation; small plus signs, reflections of pentlandite in the second orientation; weak reflections unlikely to survive reproduction of the original film have been omitted.

firming that [111]pn || [00.1]po and consequently that (111)pn || (00.1)po. The direction normal to [111]*pn in the plane of the photograph is [$\bar{1}\bar{1}$2]*pn; thus ($\bar{1}\bar{1}$2)pn || (10.0)po. In confirmation of this, zero-level precession films taken with the crystal rotated 30° about [00.1]po show parallelism of the 0$\bar{k}k$pn and *hh*.0po reciprocal lattice rows, giving (0$\bar{1}$1)pn|| (11.0)po. The orientation relationship between pentlandite and pyrrhotite is established as (111)pn|| (00.1)po, (0$\bar{1}$1)pn||(11.0)po, ($\bar{1}\bar{1}$2)pn||(10.0)po and is summarized stereographically in Figure 5.

The compositions (atomic percent) of the coexisting pyrrhotite and pentlandite in specimen 9868 are: pyrrhotite, Fe (46.01), Ni (0.62), Co (0.00), Cu (<0.01), S (53.37); pentlandite, Fe (24.72), Ni (27.68), Co (0.40), Cu (0.00), S (47.20) (Misra and Fleet, 1973a, Table 5). The lattice parameters determined from the uncalibrated precession films are: pyrrhotite (subcell), a = 3.434Å, c = 7.05Å; pentlandite, a = 10.050Å. The value for the pentlandite lattice parameter is in good agreement with that of Knop *et al.* (1965) for Creighton mine pentlandite (10.042Å).

In the earlier study (Misra and Fleet, 1974) only monoclinic pyrrhotite (4*C*) was recognized. However the present study indicates that the pyrrhotite in the vicinity of the flame pentlandite is apparently hexagonal. Careful examination of precession films

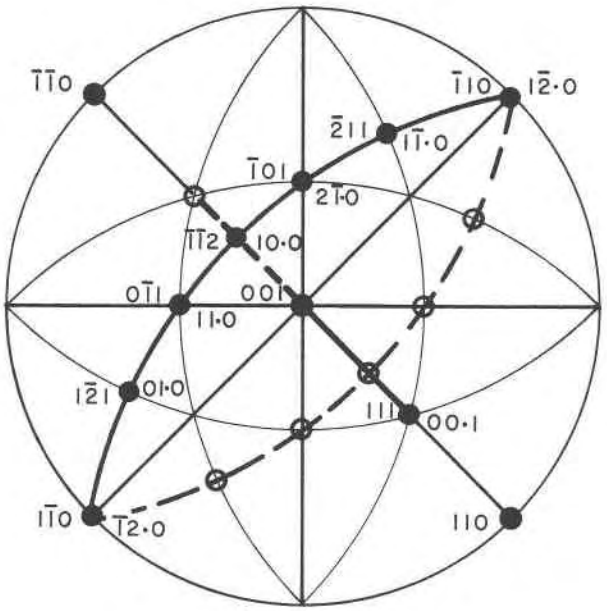

FIG. 5. Stereogram showing the orientation relationship of exsolved pentlandite (pn) in pyrrhotite (po), (111)pn (00.1)po, $(0\bar{1}1)$pn ||(11.0)po, and $(\bar{1}\bar{1}2)$pn||(10.0)po. Pentlandite indices are on the left-hand side of the poles, pyrrhotite indices on the right.

shows that, in each of the three 'equivalent' settings about the pyrrhotite *c*-axis, the distribution of the 4*C* superstructure reflection intensities has *mm* symmetry, and the pentlandite and pyrrhotite retain the parallelism of their orientation relationship. Thus, this 4*C* superstructure is the hexagonal 2*A*, 4*C* one reported by Fleet (1968).

Synthetic samples

Crystals were synthesized by evacuated silica tube techniques (Kullerud, 1971) in Kanthal-wound furnaces. A monosulfide solid-solution composition (Fe:Ni:S = 53:10:37 weight percent) was prepared by direct reaction of high-purity (99.999 percent) sulfur (ASARCO), iron (United Mineral), and nickel (Johnson, Matthey and Company, Ltd.); the iron and nickel had previously been reduced at >700°C in a stream of hydrogen. Initial reaction in evacuated silica tubes at 600°C for twenty-four hours resulted in discrete beads of $Fe_{1-x}S$ and $Ni_{1-x}S$. These were ground under acetone and then annealed in evacuated tubes for an additional twenty-four hours to homogenize the mixture. Single crystals suitable for X-ray precession studies were obtained by suspending a 3 cm long silica tube containing the homogenized powder in a vertical furnace at temperatures in excess of 900°C for one week. Crystals grew by sublimation in a thermal gradient of 5°/cm. The resulting single crystals and crystal clusters were euhedral for the most part and averaged about 0.1 mm in diameter. The presence of well-developed pinacoids (00.1) and first order dipyramids (*h*0.1) facilitated orienting the crystals on the precession camera.

Polished sections of crystals that had subsequently been annealed at 400°C for one week clearly show exsolved pentlandite. The pentlandite (~8 modal percent) occurs predominantly along cracks, edges, and grain boundaries as small oriented flame-like lamellae which coalesce to form irregular grains, and in some instances completely rim a crystal. Larger lamellae often occur within grains. Generally, the larger the pentlandite grain or lamella the more irregular its shape.

The unit-cell dimensions of the monosulfide solid-solution were refined using the least-squares program of Appleman and Evans (1973). Average *d*-values were measured from diffractometer tracings recorded with monochromatized Cu$K\alpha$ radiation from 24° to 75° 2θ, scanning at a rate of 0.5° 2θ per minute. Barium fluoride (a = 6.1971Å) was used as an internal standard.

The crystals quenched from above 900°C have a = 3.449(1)Å and c = 5.758(2)Å, where the number in parentheses is the estimated standard deviation. These values are statistically identical to the cell dimensions of the crystals that had been annealed at 400°C. Although distinct in polished sections and precession photographs, there is not sufficient pentlandite in the annealed crystals to be recorded on the diffractometer tracings. Thus, it is not surprising that no expression of nickel loss is apparent in the monosulfide solid-solution cell dimensions. Furthermore, in this compositional region of the solid-solution, unit-cell dimensions are not a particularly sensitive measure of nickel loss, since the increase in c due to the decrease in Ni is compensated by the decrease in c due to the decrease in total metal content. The cell dimension of pentlandite [a = 10.15(2)Å] was computed from measurements of precession photographs. This value corresponds to an iron-rich composition (34 atomic percent Fe) (Misra and Fleet, 1973b) as would be expected from the known phase relations (Misra and Fleet, 1973a).

Precession photographs of crystals that had been quenched in air from above 900°C were recorded about the [00.1] and [10.0] axes using Mo$K\alpha$ radiation. Neither these photographs nor those of the annealed crystals show pyrrhotite superstructure reflections. Precession photographs of the annealed

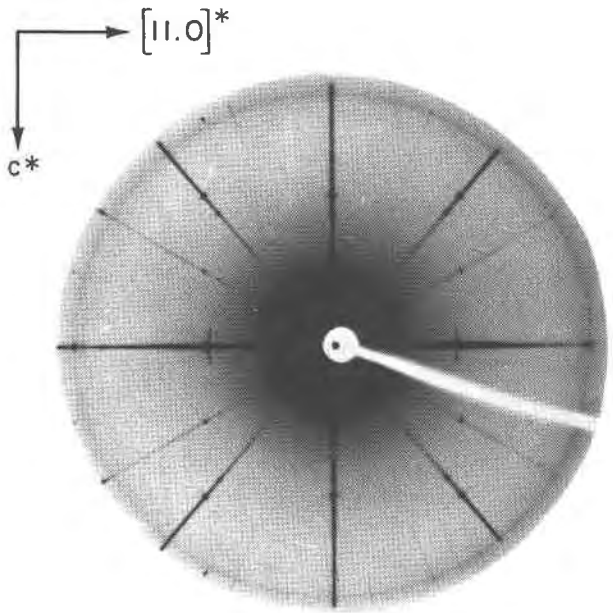

FIG. 6. Zero-level precession photograph showing crystallographic orientation of pyrrhotite and exsolved pentlandite in a synthetic crystal. [10.0]po precession axis; μ = 25°; unfiltered MoK radiation, 35 kV, 16 mA, 100 hrs. exposure. Small "powder" arcs represent pentlandite lamellae slightly misaligned with respect to the pyrrhotite host.

crystals exhibit short arc-shaped pentlandite diffractions superimposed on the pyrrhotite reciprocal lattice. The pentlandite diffractions describe arcs of about 1½° on either side of [11.0]* in the a–b plane and 8½° about the same direction in the [110]*–c*plane. The 5.88Å pentlandite d-value measured along c* of pyrrhotite is in close agreement with the published value of 5.86Å for d_{111} of iron-rich pentlandite (Misra and Fleet, 1973b). Likewise, the 3.58Å pentlandite d-value measured along [11.0]* of pyrrhotite is in good agreement with the value of 3.59Å for d_{022} of pentlandite. Indexing of these pentlandite d-values is unequivocal, as no other permitted diffractions of pentlandite or pyrrhotite correspond to these d-values. The colinearity of [111]*pn with [00.1]*po and [001]*pn with [11.0]*po fixes the mutual crystallographic orientation of these intergrown structures. In terms of the direct lattice (111)pn||(00.1)po, and (011)pn||(11.0)po.

Discussion

The same orientation relationship has been established for both natural and synthetic exsolution intergrowths of pentlandite and pyrrhotite. This corrects the orientation previously reported by Francis (1974) and Francis *et al.* (1974). The orientation relationship here established for intergrowths is not the same orientation relationship that Ehrenberg (1932) determined for epitaxial overgrowths of pentlandite on pyrrhotite. Since intergrowths are constrained in three dimensions rather than two and since more than one mutual orientation may be possible, intergrowths and overgrowths need not in general be governed by the same orientation relationship. In this case, however, if the crystals comprising the pentlandite stars in Figure 2 are interpreted as octahedra rather than dodecahedra, then the orientation relation of the overgrowths is identical to that of the intergrowths. We prefer this interpretation because it is consistent with the octahedral morphology of synthetic pentlandite crystals (C.T. Prewitt, personal communication, 1974).

Since pentlandite and pyrrhotite form oriented intergrowths, it is reasonable to infer close dimensional and structural similarities. The crystal structure of pyrrhotite is a metal-deficient derivative of the simple hexagonal NiAs-type structure (space group $P6_3/mmc$, Fig. 7). The sulfur atoms are arranged in hexagonal close-packed arrays parallel to (00.1), with metal atoms occupying the octahedral interstices. There are two formula units of $(Fe,Ni)_{1-x}S$ per unit cell. The ideal crystal structure of pentlandite (space group $Fm3m$) is based on cubic close-packed arrays

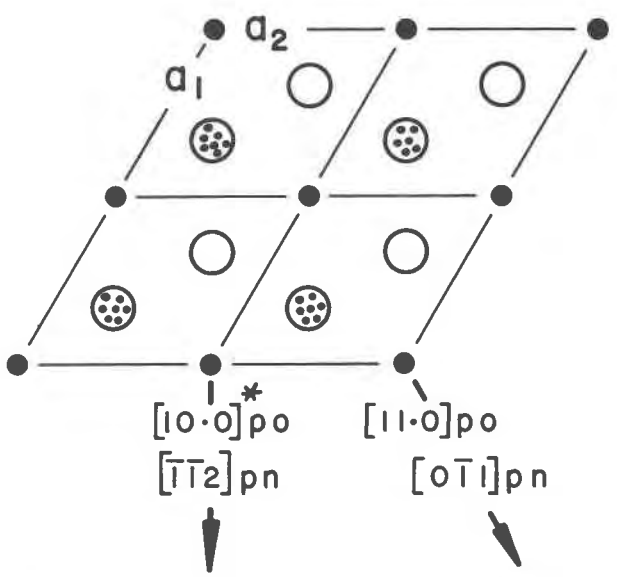

FIG. 7. Idealized structure of the pyrrhotite subcell projected parallel to c axis. Large stippled circles, S at z = 3/4; large open circles, S at z = 1/4; small solid circles, Fe at z = 0, 1/2. The orientation relationship is indicated by vectors.

of sulfur atoms parallel to (111), with metal atoms in both tetrahedral and octahedral interstices (a useful diagrammatic representation is given in Misra and Fleet, 1974, Fig. 5). In each unit cell there are four formula units of $(Fe,Ni)_9S_8$; thirty-two of the metal atoms are in tetrahedral coordination with S and four are in octahedral coordination. The average sulfur–sulfur distance in the close-packed layers of pentlandite is 3.46Å, identical to that in pyrrhotite, and the interplanar spacings normal to the close-packed layers of both structures are within two percent of one another.

Orientation of the phase boundaries between pentlandite and pyrrhotite is not fixed by establishing the mutual orientation of the respective lattices, although certain planes may become energetically favored. The precise optical determination of the phase boundary orientation is difficult because these minerals do not form the long, sharp contacts characteristic of other exsolved pairs (*e.g.* cubanite–chalcopyrite), but the weight of textural evidence (Ramdohr, 1969), albeit not rigorously determined, supports the view that pentlandite lamellae exsolved parallel to (00.1) of pyrrhotite. However, the snowflake-like illustration in Ehrenberg (1932) suggests that in at least some instances pentlandite exsolves along pyramidal pyrrhotite planes.

It is not fortuitous that the pentlandite–pyrrhotite phase boundary commonly parallels the close-packed sulfur layers. The close dimensional fit and the stacking continuity across the phase boundary produce a coherent interface parallel to the close-packed layers. Thus pentlandite forms as coherent lamellae along (00.1) planes of pyrrhotite in conformity with the criteria for oriented intergrowths recognized by Gruner (1929) and rationalized by Buerger (1934, 1945).

Pentlandite exsolves from pyrrhotite with one [111]pn axis parallel to [00.1]po. The [111]pn is a 3-fold axis whereas [00.1]po is a 6-fold axis. Thus two orientations of pentlandite, related either by reflection on $(\bar{1}12)$pn or by 2-fold rotation about [111]pn are predicted and two are observed on precession photographs (Fig. 4). The reflections of the second orientation are much weaker than those of the first, suggesting that within the volume of the sample analyzed the two orientations did not nucleate with equal probability. The two orientations are not resolved on zero-level precession photographs precessed about [01.0]po, [10.0]po, and [11.0]po since these axes are normal to the twin planes or the twin axis.

The transformation of pyrrhotite to pentlandite involves substantial changes in both crystal structure and chemical composition. For constant sulfur contents the volume change is about 9 percent, based on the lattice parameters of the natural crystal. Also, transformation of the sulfur arrays from hexagonal to cubic close-packing, assuming no cooperative mechanism, requires redistribution of shuffling of 4 out of every 6 sulfur layers. Thus the departure from parallelism shown by the arcs on the precession photograph of the synthetic crystal (Fig. 6) is not surprising. It is surprising, however, that no such departure can be detected in the natural sample. The radial displacement of reflections in Figure 4a is due merely to mechanical disruption on removal of the crystal fragment from the polished section, since the pentlandite and pyrrhotite reflections are displaced by corresponding amounts.

In subsequent experiments (Francis, 1974) monosulfide solid-solution crystals with a wide range of nickel-to-iron ratios have been synthesized. Crystals quenched from 600°C into ice water as well as those quenched in air contain 0.5–5 micron blebs of pentlandite. The presence of complete powder rings of pentlandite on precession photographs establishes their random orientation. During one experiment a fuse blew out and the furnace cooled from 600°C to room temperature in about ten hours. The crystals that experienced this slow cooling contain pentlandite in oriented lamellae rather than randomly oriented blebs. Thus pentlandite exsolution textures are dependent on cooling rate. An investigation of reaction kinetics, similar to that by Yund and Hall (1970) on pyrite exsolution of pyrrhotite, would contribute significantly to understanding the exsolution of pentlandite from pyrrhotite.

Acknowledgments

Specimens of natural pentlandite assemblages, including the Creighton mine specimen 9868, were obtained mostly from the Suffel Collection of the University of Western Ontario. Other specimens were obtained from Dr. R. Ruchan and Mr. J. Holland of the Falconbridge Nickel Mines Ltd. Original photographs of the Miggiandone specimen were kindly provided by Professor P. Randohr. Discussion with L. A. Taylor and reviews by G. V. Gibbs and D. A. Hewitt were helpful. The authors are particularly indebted to associate editor C. W. Burnham for his suggestions and diplomacy. C. A. F. was supported by a Walter S. Varr fellowship administered by the Horace Smith Fund (Springfield, Massachusetts). Experimental facilities were made possible by National Science Foundation Grant DES74-22684 to J. R. C; M. E. F. and K. C. M. were supported by an NRC operating grant. M. E. F.'s contribution to the preparation of the manuscript was made whilst on sabbatical leave at the Department of Mineralogy and Petrology, University of Cambridge, using facilities kindly made available by Professor W. A. Deer. We acknowledge gratefully these contributions to this study.

References

ALSÉN, N. (1925) Rontgenographische Untersunchung der Kristallstrukturen von Magnetkies, Breithauptit, Millerit und verwandten Verbindungen. *Geol. Foren. Stockholm Forh.* **47,** 26–62.

APPLEMAN, D. E. AND H. T. EVANS, JR. (1973) Job 9214: Indexing and least-squares refinement of powder diffraction data. *Natl. Tech. Inf. Serv.*, U.S. Dept. Commer., Springfield, Virginia, Document **PB 216 188.**

BUERGER, M. J. (1934) The temperature-structure-composition behavior of certain crystals. *Natl. Acad. Sci. Proc.* **20,** 444–453.

——— (1945) The genesis of twin crystals. *Am. Mineral.* **30,** 469–482.

CRAIG, J. R. (1973) Pyrite–pentlandite assemblages and other low temperature relations in the Fe–Ni–S system. *Am. J. Sci.* **273A,** 496–510.

——— AND G. KULLERUD (1969) Phase relations in the Cu–Fe–Ni–S system and their application to magmatic ore deposits. *Econ. Geol. Monogr.* **4,** 344–358.

EHRENBERG, H. (1932) Orientierte Verwaschsungen von Magnetkies und Pentlandite. *Z. Kristallogr.* **82,** 309–315.

FLEET, M. E. (1968) The superstructures of two synthetic pyrrhotites. *Can. J. Earth Sci.* **5,** 1183–1185.

FRANCIS, C. A. (1974) *A crystallographic study of the FeS–NiS monosulfide solution.* Master's Thesis, Virginia Polytechnic Institute and State University, Blacksburg, Virginia.

———, J. R. CRAIG AND G. V. GIBBS (1974) Crystallographic relationships in pentlandite exsolution (abstr.). *Geol. Soc. Am. Abstr. Programs,* **6,** 741.

GRUNER, J. W. (1929) Structural reasons for oriented intergrowths in some minerals. *Am. Mineral.* **14,** 227–237.

HARALDSEN, H. (1941) Uber die Hochtemperaturumwandlungen der Eisen (II) sulfidmischkristalle. *Anorg. Chem.* **246,** 195–226.

HAWLEY, J. E. AND V. A. HAW (1957) Intergrowth of pentlandite and pyrrhotite. *Econ. Geol.* **56,** 467–487.

HEWITT, R. L. (1938) Experiments bearing on the relation of pyrrhotite to other sulphides. *Econ. Geol.* **33,** 305–338.

KNOP, O. AND M. A. IBRAHIM (1961) Chalcogenides of the transition elements. II. Existence of the *TT* phase in the M_9S_8 section of the system Fe–Co–Ni–S. *Can. J. Chem.* **39,** 297–317.

———, ——— AND SUTARNO (1965) Chalcogenides of the transition elements. IV. Pentlandite, a natural π phase. *Can. Mineral.* **8,** 291–316.

KULLERUD, G. (1956) Subsolidus phase relations in the Fe–Ni–S system. *Carnegie Inst. Wash. Year Book,* **58,** 175–180.

——— (1962) The Fe–Ni–S system. *Carnegie Inst. Wash. Year Book,* **61,** 144–150.

——— (1971) Experimental techniques in dry sulfide research. In, G. C. Ulmer, Ed., *Research Techniques for High Pressures and High Temperatures.* Springer-Verlag, New York, p. 289–315.

LUNDQVIST, D. (1947) X-ray studies on the ternary system Fe–Ni–S. *Arkiv Kemi, Mineral. Geol.* **24A,** No. 22, 12 p.

LINDQVIST, M., D. LUNDQVIST AND A. WESTGREN (1936) The crystal structure of Co_9S_8 and pentlandite $(Ni, Fe)_9S_8$. *Kemi Tidskr. (Stockholm),* **48,** 156–160.

MISRA, K. C. (1972) *Phase relations in the Fe–Ni–S system.* Ph.D. Thesis, University of Western Ontario, London, Canada.

——— AND M. E. FLEET (1973a) The chemical composition of synthetic and natural pentlandite assemblages. *Econ. Geol.* **68,** 518–139.

——— AND——— (1973b) Unit cell parameters of monosulfide, pentlandite, and taenite solid solutions within the Fe–Ni–S system. *Mater. Res. Bull.* **8,** 669–678.

——— AND ——— (1974) Chemical composition and stability of violarite. *Econ. Geol.* **59,** 391–403.

NALDRETT, A. J. AND G. KULLERUD (1967) A study of the Strathcona mine and its bearing on the origin of nickel–copper ores of the Sudbury district, Ontario. *J. Petrol.* **8,** 453–531.

———, J. R. CRAIG AND G. KULLERUD (1967) The central portion of the Fe–Ni–S system and its bearing on pentlandite exsolution in iron–nickel sulfide ores. *Econ. Geol.* **62,** 827–847.

NEWHOUSE, W. H. (1927) Equilibrium relations of pyrrhotite and pentlandite. *Econ. Geol.* **22,** 283–300.

PEARSON, A. D. AND M. J. BUERGER (1956) Confirmation of the crystal structure of pentlandite. *Am. Mineral.* **41,** 804–805.

RAJAMANI, V. AND C. T. PREWITT (1973) Crystal chemistry of the natural pentlandites. *Can. Mineral.* **12,** 178–187.

RAMDOHR, P. (1969) *The ore minerals and their intergrowths.* Pergamon Press. New York, 1174 p.

SHEWMAN, R. W. AND L. A. CLARK (1970) Pentlandite phase relations in the Fe–Ni–S system and notes on the monosulfide solutions. *Can. J. Earth. Sci.* **7,** 67–85.

YUND, R. A. AND H. T. HALL (1970) Kinetics and mechanism of pyrite exsolution from pyrrhotite. *J. Petrol.* **11,** 381–404.

Manuscript received, December 19, 1975; accepted for publication, April 26, 1976.